TriboBR
First International Brazilian Conference on Tribology – TriboBr-2010 and ITS - IFToMM 2010 - 2nd International Tribology Symposium of IFToMM
24th to 26th november, 2010
Copacabana, Rio de Janeiro/RJ, Brazil
ISSN 2179-3956

STABILITY CHARATERISTICS OF A TRI-TAPER JOURNAL BEARING: A LINEARIZED PERTURBATION APPROACH[1]

Raghuvir Pai[2]
D. Shrikanth Rao[2]
B. Satish Shenoy[3]
Rammohan S.Pai[4]

Abstract
In this paper, the stability characteristics of a tri-taper journal bearing is analyzed theoretically. The time dependent form of Reynolds equation in two dimensions for incompressible fluid is solved numerically by finite difference method, satisfying the Reynolds boundary conditions. Dynamic coefficients are determined using the method of linearization of bearing reactions. A study with various ramp size's and L/D ratio's predicts that a bearing with higher ramp size and higher L/D ratio results in an increased mass parameter and improved stability margin of the bearing.
Key words: Fluid film bearing; Linearized bearing reactions; Stiffness and damping; Stability; Tri-taper journal bearing.

[1] *Technical contribution to the First International Brazilian Conference on Tribology – TriboBr-2010, November, 24th-26th, 2010, Rio de Janeiro, RJ, Brazil.*
[2] *Professor*
[3] *Reader,Department of Mechanical and Manufacturing Engineering, Manipal Institute of Technology, Manipal, Karnataka, India-576104.*
[4] *Head, Department of Aeronautical and Automobile Engineering, Manipal Institute of Technology, Manipal, Karnataka, India-576104.*

ISSN 2179-3956

1 INTRODUCTION

Circular fluid film bearings can only offer a little improvement on the stability of rotor bearing systems. Attention was therefore directed on non-circular forms like lemon bore, offset half, pressure dam and bearings by Akkok, McC and Ettles,[1] ,Schuller,[2,3] Malik, Chandra and Sinhasan.[4,5] The notable feature of all these types is their contribution to an improvement in performance and therefore is called the anti-whirl, multi-film bearings. Hargreaves[6] did the first study dealing with the tri-taper bearing, which predicted the influence of manufacturing tolerances, misalignment as well as turbulence on the steady state performance of a tri-taper journal bearing. His study concluded that over-sized ramps results in an increased oil flow rate and a decreased load-carrying capacity. Rao *et al.,*[7] made a comparative study on the effect of Reynolds and JFO cavitation boundary condition on the steady state performance of a tri-taper journal bearing. Theoretical investigations are carried out by Rao *et al.*[8] to ascertain the whirl instability of a rotor supported on a tri-taper journal bearing, operating under steady, periodic and variable rotating load, using non-linear transient approach as given by Majumdar and Brewe.[9] The dynamic equations of motion are solved by fourth-order Runge–Kutta method to result in eccentricity ratio, attitude angle and their derivatives, which is used for the next time step. Hydro- dynamic forces are then evaluated using these values in the time-dependent Reynolds equation in two dimensions for incompressible fluid. Stability of the rotor bearing system is determined from the journal locus. In this paper, a linearized perturbation approach is used to study the stability characteristics of tri-taper journal using the Reynolds boundary condition. The time-dependent Reynolds equation in two dimensions is solved for this purpose. A first order perturbation method is used to find the dynamic pressures in the clearance space. The stiffness and damping coefficients (both direct and cross components) are calculated from the real and imaginary parts of the integrated pressures. These coefficients are then used in the equations of motion of a rigid rotor for estimating the mass parameter, a measure of stability. The effect of ramp size and L/D ratio on the stability of these bearings is studied. The results are in dimensionless form and can be conveniently used in the design of these bearings.

2 BEARING GEOMETRY

Geometrical arrangement of a tri-taper bearing is similar to that of a three-lobe journal bearing. However, this bearing is akin to three tapered land composite thrust bearings arranged around a bearing circle. There are three lubricant supply grooves, equi-spaced at 120^0 apart, around the bearing periphery. Each of the three sections consists of equal lengths of the bearing base circle and a section offset from the base circle, such that, it merges smoothly with the base circle and provides a predetermined depth at or near to the lubricant supply groove. The sectional view of the tri-taper journal bearing is shown in Figure 1.

ISSN 2179-3956

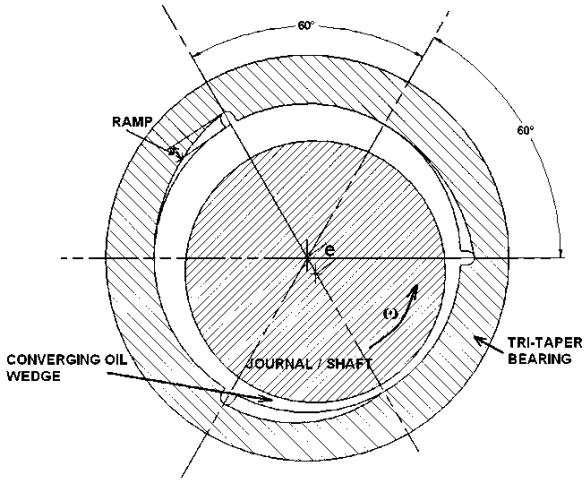

Figure 1. Sectional view of the tri-taper journal bearing.

3 THEORY

The basic differential equation for pressure distribution in the bearing clearance under dynamic conditions for incompressible fluid may be written as

— — — — —

The lubricant film profile is determined by superimposing the effect of ramp on the conventional expression for the film thickness. Film thickness equation for all configurations of the bearing can be given by

(2)

Using the following substitutions

– – —— –

Equation (1) can be non-dimensionlized as:

— — – – — — —

Where

— ——— — ———

4 PRESURE BOUNDARY CONDITION

Pressure along the bearing edges was set to zero.
$\overline{p}_0 = 0.0$ at $\overline{z} = 0$ and $\overline{z} = 1$ for all θ

ISSN 2179-3956

Cavitation was allowed to occur at ambient pressure by setting all calculated negative pressure equal to zero through out the iterative solution scheme. This implies that the lubricant film ruptures and reforms when

$$\bar{p} = 0, \ \partial\bar{p}/\partial\theta = 0$$

The non dimensionlized supply pressure $\bar{p}_s = 0.1362$ was set at the grooves.

5 STEADY STATE CHARACTERISTICS

Under steady state conditions, the time-dependent term is dropped. The governing equation will then be:

$$\frac{\partial}{\partial\theta}\left(\bar{h}_0^3\frac{\partial\bar{p}_0}{\partial\theta}\right) + \frac{1}{4}\left(\frac{D}{L}\right)^2\bar{h}_0^3\frac{\partial^2\bar{p}_0}{\partial\bar{z}^2} = 6\frac{d\bar{h}_0}{d\theta} \tag{4}$$

In the conventional cylindrical bearing the coordinate θ in the circumferential direction is taken from the position of maximum film thickness. In the grooved bearing this position needs to be found before hand. This is done by assuming an arbitrary value of attitude angle ψ and the coordinate θ^* is measured from the vertical position. Using this ψ the film thickness is obtained from equation (2) and equation (4) is solved for pressure using the boundary conditions. The force components along and perpendicular to the line of centres are found from:

$$\bar{W}_r = \frac{W_r C^2}{\eta U R^2 L} = -\int_0^1\int_0^{2\pi}\bar{p}_0\cos(\theta^* - \psi)\,d\theta\,d\bar{z} \tag{5}$$

$$\bar{W}_t = \frac{W_t C^2}{\eta U R^2 L} = \int_0^1\int_0^{2\pi}\bar{p}_0\sin(\theta^* - \psi)\,d\theta\,d\bar{z} \tag{6}$$

The load capacity and attitude angle are

$$\bar{W} = [\bar{W}_r^2 + \bar{W}_t^2]^2 \tag{7}$$

$$\phi_0 = tan^{-1}\left(\frac{\bar{W}_t}{\bar{W}_r}\right) \tag{8}$$

After each calculation, the attitude angle calculated from equation (8) is compared with the assumed value of attitude angle (ψ). The value of ψ is modified with a small increment of ψ and the Reynolds equation is solved using this modified value until ψ is equal to Φ_0.

6 DYNAMIC CHARACTERISTICS

The Reynolds equation under dynamic conditions , equation (3) is solved assuming that the journal performs a periodic motion of small amplitude $Re(C\varepsilon_1 e^{i\tau})$ along the line of centres and $Re(C\varepsilon_0\Phi_0 e^{i\tau})$ perpendicular to the line of centres around its steady state position ε_0 and Φ_o. It is assumed at the onset of instability, the position of the journal centre can be defined as a steady state value (ε_0, Φ_o) together with a harmonic vibration of frequency ω_p, Thus

$$\epsilon = \epsilon_0 + \epsilon_1 e^{i\tau}$$
$$\phi = \phi_0 + \phi_1 e^{i\tau}$$

ISSN 2179-3956

where

$$|\epsilon_1| \ll \epsilon_0$$
$$|\phi_1| \ll \phi_0$$

Under this condition (i.e. for a small amplitude of vibration) first-order perturbation will be valid.
The pressure and film thickness can be written as

$$\bar{p} = \bar{p}_0 + \epsilon_1 e^{i\tau}\bar{p}_1 + \epsilon_0\phi_1 e^{i\tau}\bar{p}_2 \quad (9)$$
$$\bar{h} = \bar{h}_0 + \epsilon_1 e^{i\tau}\cos\theta + \epsilon_0\phi_1 e^{i\tau}\sin\theta \quad (10)$$

Substitution of equations (9) and (10) in equation (3) and retaining up to first linear terms gives the following equations

$$\left(\bar{h}_0^3\frac{\partial^2\bar{p}_0}{\partial\theta^2}\right) + 3\bar{h}_0^2\frac{\partial\bar{h}_0}{\partial\theta}\frac{\partial\bar{p}_0}{\partial\theta} + \frac{1}{4}\left(\frac{D}{L}\right)^2\bar{h}_0^3\frac{\partial^2\bar{p}_0}{\partial\bar{z}^2} - 6\frac{d\bar{h}_0}{d\theta} = 0 \quad (11)$$

$$\left(\bar{h}_0^3\frac{\partial^2\bar{p}_1}{\partial\theta^2}\right) + 3\bar{h}_0^2\cos\theta\frac{\partial^2\bar{p}_0}{\partial\theta^2} - 3\bar{h}_0^2\sin\theta\frac{\partial\bar{p}_0}{\partial\theta} + 6\bar{h}_0\cos\theta\frac{\partial\bar{h}_0}{\partial\theta}\frac{\partial\bar{p}_0}{\partial\theta} + 3\bar{h}_0^2\frac{\partial\bar{h}_0}{\partial\theta}\frac{\partial\bar{p}_1}{\partial\theta} + \frac{1}{4}\left(\frac{D}{L}\right)^2\bar{h}_0^3\frac{\partial^2\bar{p}_1}{\partial\bar{z}^2} + \frac{3}{4}\left(\frac{D}{L}\right)^2\bar{h}_0^2\cos\theta\frac{\partial^2\bar{p}_0}{\partial\bar{z}^2} + 6\sin\theta - 12i\lambda\cos\theta = 0 \quad (12)$$

$$\left(\bar{h}_0^3\frac{\partial^2\bar{p}_2}{\partial\theta^2}\right) + 3\bar{h}_0^2\sin\theta\frac{\partial^2\bar{p}_0}{\partial\theta^2} - 3\bar{h}_0^2\cos\theta\frac{\partial\bar{p}_0}{\partial\theta} + 6\bar{h}_0\sin\theta\frac{\partial\bar{h}_0}{\partial\theta}\frac{\partial\bar{p}_0}{\partial\theta} + 3\bar{h}_0^2\frac{\partial\bar{h}_0}{\partial\theta}\frac{\partial\bar{p}_2}{\partial\theta} + \frac{1}{4}\left(\frac{D}{L}\right)^2\bar{h}_0^3\frac{\partial^2\bar{p}_2}{\partial\bar{z}^2} + \frac{3}{4}\left(\frac{D}{L}\right)^2\bar{h}_0^2\sin\theta\frac{\partial^2\bar{p}_0}{\partial\bar{z}^2} + 6\cos\theta - 12i\lambda\sin\theta = 0 \quad (13)$$

Knowing the steady state pressure distribution, equations (12) and (13) are solved numerically satisfying the boundary conditions.

7 STIFFNESS AND DAMPING COEFFICIENTS

It is found that the fluid film, which supports the rotor, is equivalent to a spring and a dashpot system. Since the journal executes small harmonic oscillations about its steady state position, the dynamic load-carrying capacity can be expressed as a spring and a viscous damping force. This results in four stiffness and damping coefficients as given below-

$$\bar{K}_{rr} = -Re\left(\int_0^1\int_0^{2\pi}\bar{p}_1\cos\theta\,d\theta\,d\bar{z}\right)$$
$$\bar{K}_{\phi r} = -Re\left(\int_0^1\int_0^{2\pi}\bar{p}_1\sin\theta\,d\theta\,d\bar{z}\right)$$
$$\bar{D}_{rr} = -Im\frac{\left(\int_0^1\int_0^{2\pi}\bar{p}_1\cos\theta\,d\theta\,d\bar{z}\right)}{\lambda}$$
$$\bar{D}_{\phi r} = -Im\frac{\left(\int_0^1\int_0^{2\pi}\bar{p}_1\sin\theta\,d\theta\,d\bar{z}\right)}{\lambda} \quad (14)$$

ISSN 2179-3956

where

$$\bar{K}_{ij} = \frac{K_{ij}C}{LDp_s} \; and \; \bar{D}_{ij} = \frac{D_{ij}C\omega}{LDp_s}$$

Considering the dynamic displacement of the journal centre along the Φ direction, the following expressions result

$$\begin{aligned}
\bar{K}_{\phi\phi} &= -Re\left(\int_0^1 \int_0^{2\pi} \bar{p}_2 \sin\theta \, d\theta \, d\bar{z}\right) \\
\bar{K}_{r\phi} &= -Re\left(\int_0^1 \int_0^{2\pi} \bar{p}_2 \cos\theta \, d\theta \, d\bar{z}\right) \\
\bar{D}_{\phi\phi} &= -Im\frac{\left(\int_0^1 \int_0^{2\pi} \bar{p}_2 \sin\theta \, d\theta \, d\bar{z}\right)}{\lambda} \\
\bar{D}_{r\phi} &= -Im\frac{\left(\int_0^1 \int_0^{2\pi} \bar{p}_2 \cos\theta \, d\theta \, d\bar{z}\right)}{\lambda}
\end{aligned} \tag{15}$$

The stiffness and damping coefficients thus obtained can be used to study the stability of a rigid rotor supported on this bearing.

8 STABILITY ANALYSIS

The stability of the journal is analysed by combining the equations of motion and the film forces F_r and F_Φ , assuming the rotor to be rigid and having a mass M. The equations of motion in nondimensional form are written as-

$$\bar{M} = \frac{1}{\lambda^2(\bar{D}_{\phi\phi}+\bar{D}_{rr})}\left[\left(\bar{D}_{rr}\bar{K}_{\phi\phi} + \bar{K}_{rr}\bar{D}_{\phi\phi}\right) - \left(\bar{K}_{\phi r}\bar{D}_{r\phi} + \bar{D}_{\phi r}\bar{K}_{r\phi}\right) + \frac{W}{\varepsilon_0}\left(\bar{D}_{rr}\cos\phi_0 - \bar{D}_{\phi r}\sin\phi_0\right)\right] \tag{16}$$

$$\bar{M}^2\lambda^4 - \lambda^2\left[\bar{M}\left(\frac{\bar{W}\cos\phi_0}{\epsilon_0} + \bar{K}_{\phi\phi} + \bar{K}_{rr}\right)\left(\bar{D}_{rr}\bar{D}_{\phi\phi} - \bar{D}_{\phi r}\bar{D}_{r\phi}\right)\right] + \left(\bar{K}_{rr}\bar{K}_{\phi\phi} - \bar{K}_{\phi r}\bar{K}_{r\phi}\right) + \frac{\bar{W}}{\varepsilon_0}\left(\bar{K}_{rr}\cos\phi_0 - \bar{K}_{\phi r}\sin\phi_0\right) = 0 \tag{17}$$

Equations (16) and (17) are linear algebraic equations in $\bar{M}$ and λ and the solution of these will give $\bar{M}$ and λ. The speed of the journal calculated from this value of $\bar{M}$ is the threshold speed, above which the bearing system will be unstable. The whirl speed (speed of the journal centre) can be found from the whirl ratio for the journal speed. It must be noted that the journal centre rotates in the same direction as that of the journal.

9 RESULTS AND DISCUSSION

To validate the computer code, the dynamic characteristics namely, direct and cross stiffness and damping coefficient for a plain journal bearing are compared with those obtained by Stachowiak and Batchelor[10] for the same bearing configuration, Figure 2 and Figure 3. Hargreaves[6] has provided the design data for a tri-taper bearing operating in the turbulent regime. The results of his study has been applied to a high speed gear box, where manufacturing tolerances and misalignment have significant

ISSN 2179-3956

effects on the steady state performance of the bearings. Rao *et al.* [8] have studied the dynamic characteristics of a tri-taper bearing using a nonlinear transient method. They have obtained the journal centre locus to ascertain the stability of the bearing system for various ramp and L/D ratios and under different loading conditions. The preceding research papers have not made an attempt to use the linearized perturbation method to ascertain the stability of the bearing system. This method is not as computer intensive as a nonlinear transient method or the modeling of turbulence and misalignment. At the same time the results this study will be fairly useful. In this paper, the influence of ramp and L/D ratio on dynamic performance characteristics of a tri-taper journal bearing is studied. The computed values of direct stiffness, cross stiffness and damping co-efficient are plotted with eccentricity ratio and are presented below :

From Figure 4, the non-dimensional direct stiffness co-efficient, K_{RR}, increases with increase in eccentricity ratio for all L/D ratios and ramp sizes. The range of K_{RR} value is higher for lower L/D ratios. But for lower eccentricity ratios ($\varepsilon < 0.5$), bearing with R_{amp} = 0.58 shows lesser value of K_{RR} than a bearing with ramp size of 0 and 0.25.

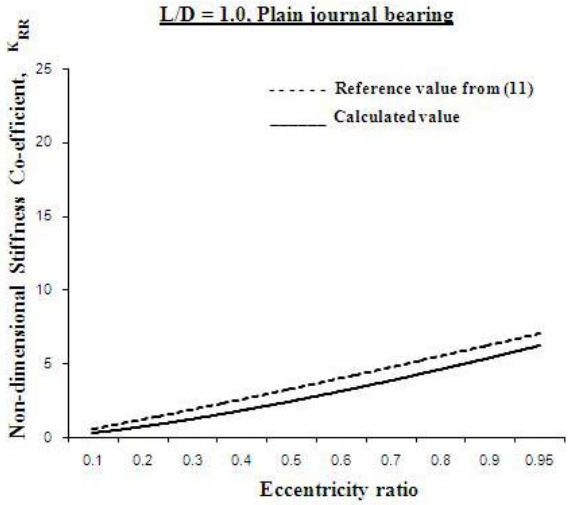

Figure 2. Comparison of Non-dimensional direct Stiffness Co-efficient.

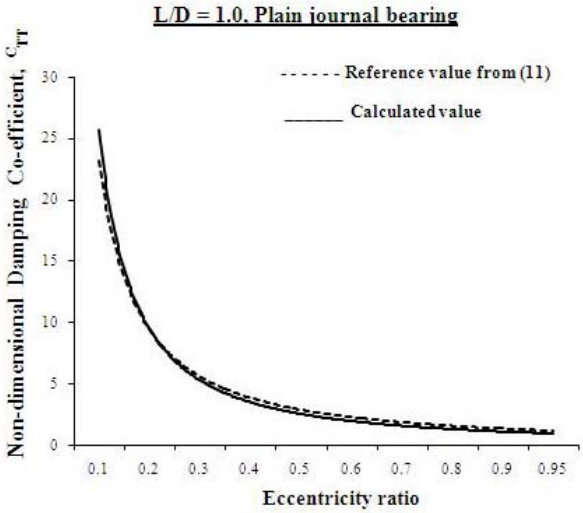

Figure 3. Comparison of Non-dimensional direct damping coefficient

ISSN 2179-3956

From Figure 5, it is observed that the range of values of non-dimensional cross stiffness co-efficient, K_{TR}, increases with increase in L/D ratio. For bearing with L/D = 1.0, or 1.225 and ramp sizes 0 and 0.25, an increase in eccentricity ratio decreases the value of K_{TR}. However, for a bearing with R_{amp} = 0.58, increase in eccentricity ratio increases the value of K_{TR}, peaks at eccentricity ratio of 0.6, and decreases with further increase in eccentricity ratio.

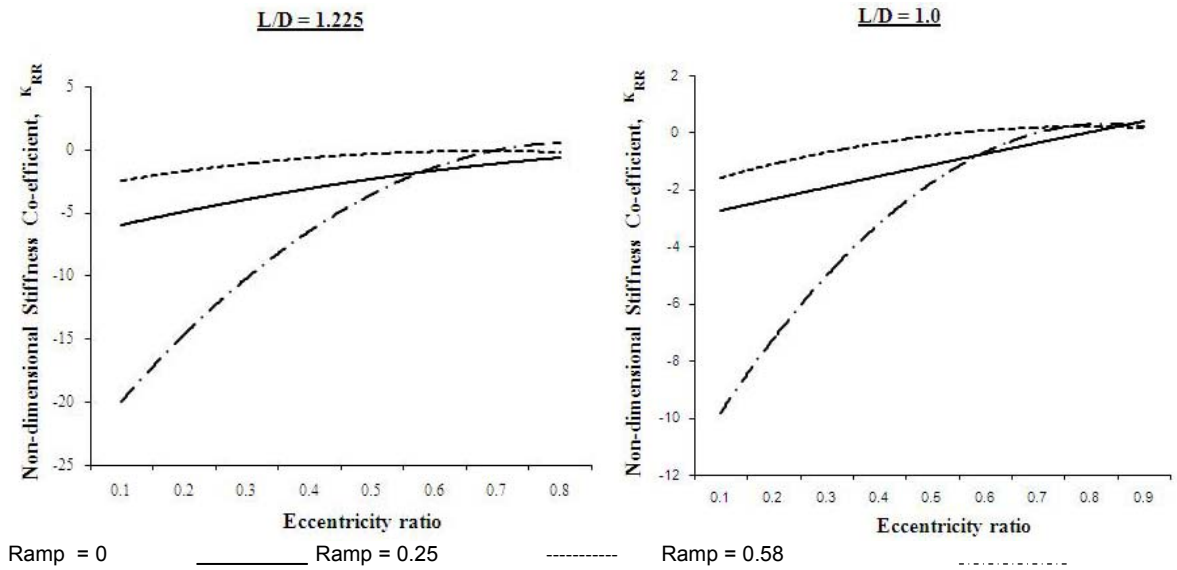

Figure 4. Comparison of Non-dimensional direct stiffness co-efficient, K_{RR} for a tri-taper bearing with different L/D ratios.

From Figure 6, it is observed that the range of values of non-dimensional direct damping co-efficient, C_{RR} decreases with increase in L/D ratio. At lower eccentricity ratios ($\varepsilon < 0.5$), bearing with R_{amp} = 0.58 has lesser value of C_{RR} than bearings with ramp size 0 and 0.25. However at higher eccentricity ratios, bearing with R_{amp} = 0.58 has higher value of C_{RR}. For L/D=1.0 or 1.225 and bearings with ramp sizes of 0 and 0.25, an increase in eccentricity ratio results in increase in the value of C_{RR}. For a bearing with R_{amp} = 0.58, the value of C_{RR} at eccentricity ratio less than 0.6 is considerably lower compared to that for a bearing of ramp size 0 and 0.25.

ISSN 2179-3956

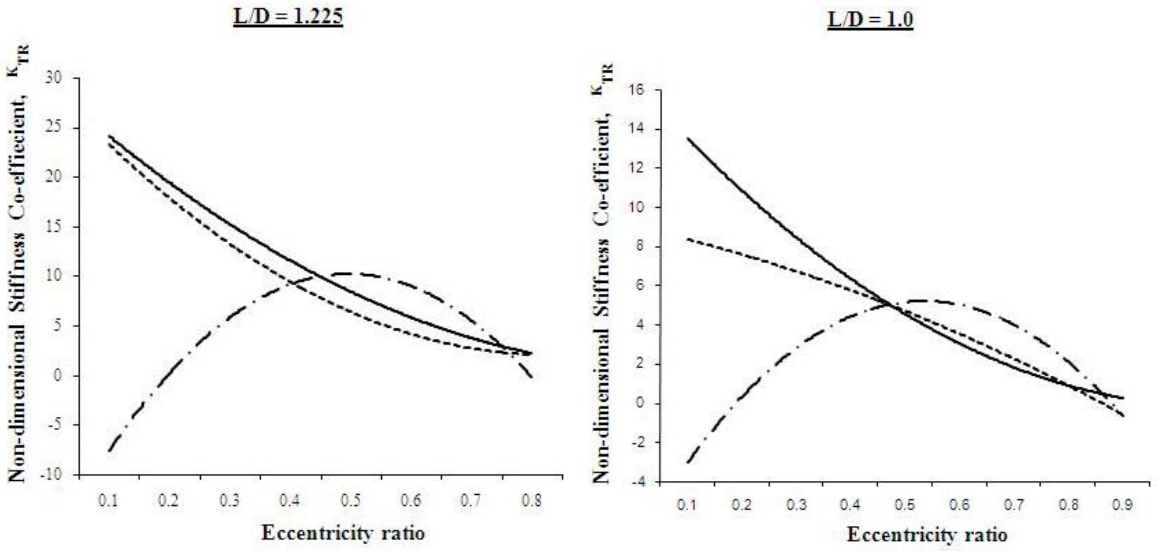

Figure 5. Comparison of Non-dimensional cross stiffness co-efficient, K_{TR} for a tri-taper bearing with different L/D ratios.

From Figure 7, it is seen that the range of values of non-dimensional direct damping co-efficient C_{TT} increases with increase in L/D ratio. For L/D = 1.0, or 1.225 as the eccentricity ratio increases, the value of C_{TT} decreases for bearings with ramp size of 0 and 0.25. For bearing with R_{amp} = 0.58, increase in eccentricity ratio results in increase in C_{TT}, attains a maximum value at eccentricity ratio of 0.6; and further increase in eccentricity decreases the value of C_{TT}. From Figure 8, it is observed that the range of values of non-dimensional cross damping co-efficient C_{TR} increases with increase in L/D ratio. For a bearing with L/D = 1.0 OR 1.225 and R_{amp} = 0 and 0.25, increase in eccentricity ratio decreases the value of C_{TR}. For a bearing with R_{amp} = 0.58, an increase in eccentricity ratio increases the value of C_{TR}, peaks at an eccentricity ratio of 0.6, and further increase in eccentricity ratio decreases the value of C_{TR}. For lower eccentricity ratio ($\varepsilon < 0.5$), the value of C_{TR} is lower for bearings with higher ramp sizes; while for higher eccentricity ratios ($\varepsilon > 0.5$), R_{amp} = 0.58 shows higher value of C_{TR} than bearings with ramp sizes of 0 and 0.25.

ISSN 2179-3956

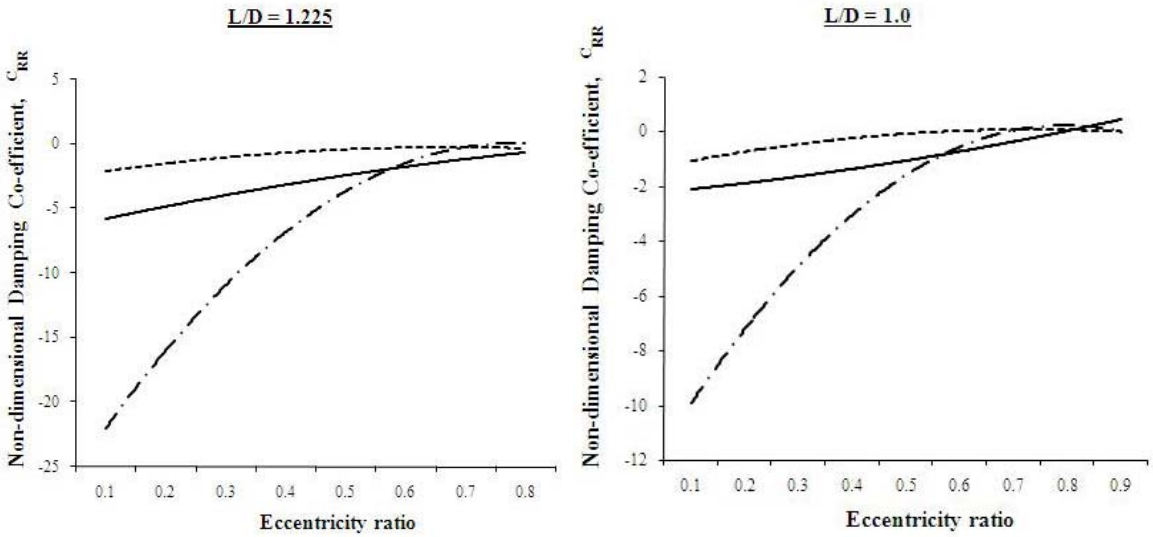

Figure 6. Comparison of Non-dimensional direct damping co-efficient, C_{RR} for a tri-taper bearing with different L/D ratios.

10 STABILITY

Clearance plays an important role in deciding bearing stability. Figure 9, shows the effect of ramp size on critical mass parameter and Figure 10, depicts its effect on whirl frequency ratio for a bearing with L/D = 1.0. The bearing with R_{amp} = 0.58 offers better stability than R_{amp} = 0.25. Figure 9, depicts that increase in the ramp size increases the critical mass parameter, resulting in an improvement in the stability margin.

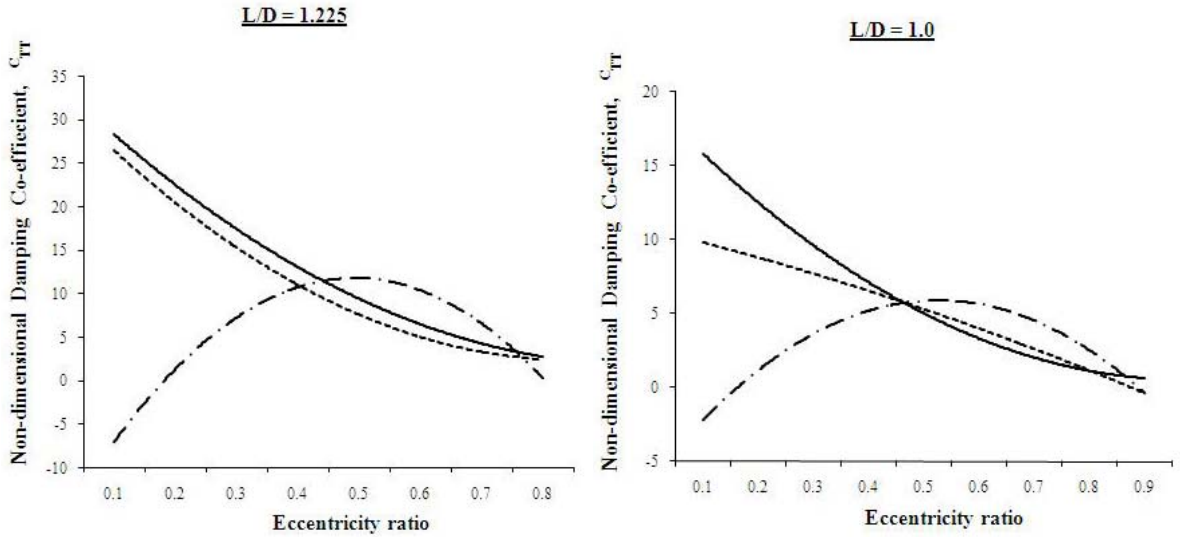

Figure 7. Comparison of Non-dimensional direct damping co-efficient, C_{TT} for a tri-taper bearing with different L/D ratios.

ISSN 2179-3956

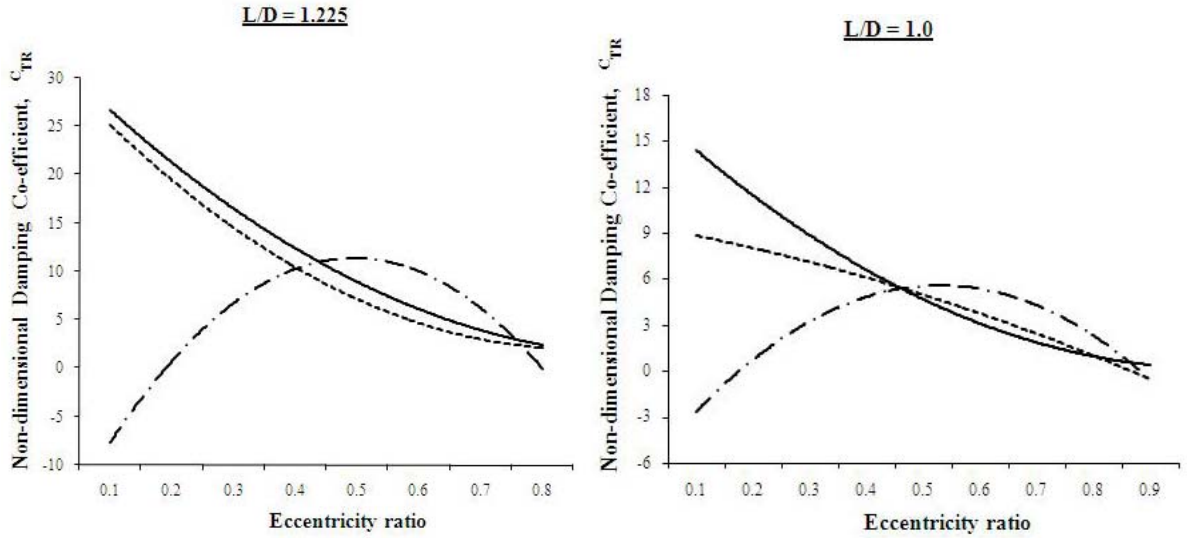

Figure 8. Comparison of Non-dimensional cross Damping co-efficient, C_{TR} for a tri-taper bearing with different L/D ratios.

11 CONCLUSIONS

It is the dynamic load characteristics of the bearings of a rotor-bearing system, which help, determine the critical speeds and the threshold of instability of the rotor-bearing system.

At higher eccentricity ratios, the ramp has least influence on values of K_{TT} and K_{TR}. Dimensionless C_{TT} is more in the case of circular bearings and dimensionless C_{RT} is more for a bearing with $R_{amp} = 0.58$. Dimensionless C_{TR} and C_{RR} is more for circular bearings at lower eccentricity ratios, however, a bearing with $R_{amp} = 0.58$ has more C_{RR} and C_{TR} at higher eccentricity ratios. Figure 9. depicts that increase in the ramp size increases the critical mass parameter, resulting in an improvement in the stability margin. Variation in film thickness significantly affects the performance characteristics of the bearing. The bearing with R_{amp} = 0.58 offers better stability than R_{amp} = 0.25.

ISSN 2179-3956

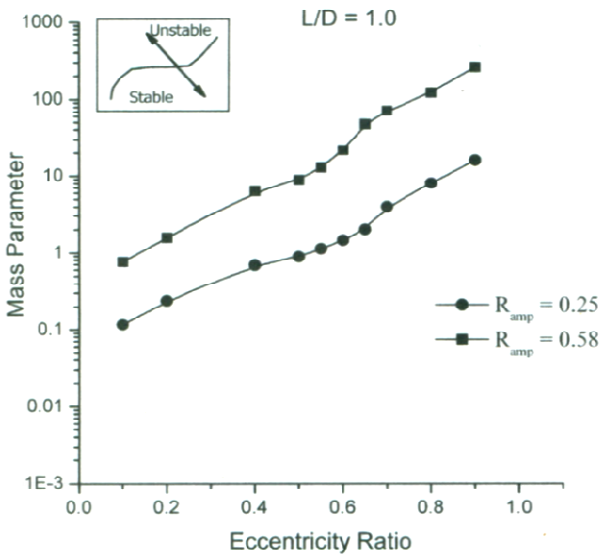

Figure 9. Critical mass parameter Vs. Eccentricity ratio for various ramp sizes.

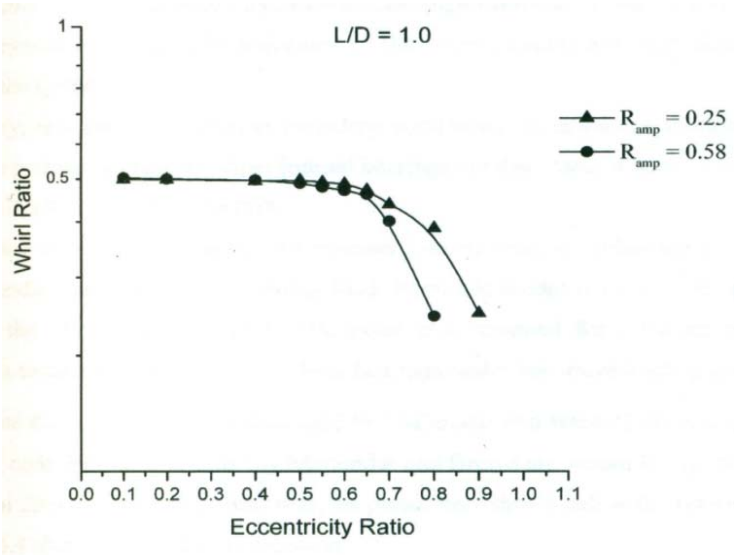

Figure 10. Whirl frequency ratio Vs. Eccentricity ratio for various ramp sizes.

REFERENCES

1 1 AKKOK, M., McC,ETTLES, C.M. The onset of Whirl instability in journal bearings of various bore shapes and groove sizes. *Transactions ASME*, v.105, p. 342–52,1983.

2 SCHULLER, F.,T. Effect of number of lobes and length–diameter ratio on the stability of tilted-lobe hydrodynamic journal bearings at zero load. *NASA TM*, D-7902:5 1975.

3 SCHULLER, F., T. Stability experiments with hydrodynamic-tilted lobe journal bearings of various number of lobes and length-to-diameter ratios. *ASLE Transactions*, v. 20, p. 271–81,1977.

4 MALIK, M., CHANDRA, M., SINHASAN, R. Performance characteristics of titled three-lobe journal bearing configurations. *Tribology International*, v.14, n. 6, p. 345–50, 1981.

5 MALIK, M., CHANDRA, M., SINHASAN, R. Design data for three-lobe bearings. *ASLE Transactions*, v.24, n. 3, p. 345–53,1981.

6 HARGREAVES, D., J. Predicted performance of a tri-taper journal bearing including turbulence and misalignment effects. *Proceedings of Institution of Mechanical Engineers, Journal of Engineering Tribology*, v. 209, Part J, p. 85–97, 1995.

ISSN 2179-3956

7 RAO, D. S., PAI, R., HARGREAVES, D. J., Static characteristics of tri-taper journal bearing. *Proceedings of the international tribology conference—AUSTRIB 2006*,QUT, Brisbane, Australia,Paper no.0109,2006.
8 RAO, D.S., SHENOY, B.S., PAI, R.S., PAI, R. Stability of tri-taper journal bearings under dynamic load using a non linear transient method. *Tribology International*, v. 43, p. 1584-1591, 2010.
9 MAJUMDAR, B. C.,BREWE, D.E. Stability of a rigid rotor supported on oil film journal bearings under dynamic load. *NASA TM*, 102309, 1987.
10 STACHOWIAK G., BATCHELOR, A., Engineering Tribology. *Butterworth-Heinemann, Elsevier Tribology Series,* September, 2005.

Nomenclature

C -radial clearance (m)

D-diameter of the bearing (m)
D_{rr} $D_{\Phi\Phi}$ $D_{r\Phi}$ $D_{\Phi r}$ – Damping coefficients
$\bar{D}_{rr}\bar{D}_{\phi\phi}\bar{D}_{r\phi}\bar{D}_{\phi r}$ - Non-dimensional damping coefficient, $\bar{D}_{ij} = \frac{D_{ij}C\omega}{LD\,p_s}$
R-radius of the bearing (m)
e-eccentricity (m)
F_r ,$\bar{F}_r$ dynamic force along radial direction,$\bar{F}_r = \frac{F_r C^2}{\eta\omega R}$
F_Φ,$\bar{F}_\phi$ dynamic forcealong f direction, $\bar{F}_\Phi = \frac{F_\Phi C^2}{\eta\omega R}$
h,$\bar{h}$ local film thickness(m), $\bar{h} = \frac{h}{C} = 1 + \varepsilon\cos\theta + Ramp$
K_{rr} $K_{\Phi\Phi}$ $K_{r\Phi}$ $K_{\Phi r}$ – Damping coefficients
$\bar{K}_{rr}\bar{K}_{\phi\phi}\bar{K}_{r\phi}\bar{K}_{\phi r}$ - Non-dimensional damping coefficient, $\bar{K}_{ij} = \frac{K_{ij}C\omega}{LD\,p_s}$
R_{amp}-Normalized ramp size, Ramp/C
L- length ofthebearing (m)
M,$\bar{M}$ - mass parameter (kg), $\bar{M} = \frac{MC^3\omega^2}{\eta UR^2L}$
p,$\bar{p}$ film pressure(N/m^2), $\bar{p} = \frac{pC^2}{\eta\omega R^2}$
$\bar{p}_s$ - non-dimensional supply pressure
$\bar{p}_a$ - pressure at the bearing edges
$\bar{p}_1, \bar{p}_2$ - perturbed pressures
t - time (s)
U- journal peripheral speed, ωR (m/s)
W- steady state load capacity (N)
$\bar{W}$ -non-dimensional load capacity, $\bar{W} = WC^2/\eta UR^2L$
$W_{r,t}$ –components of load along and perpendicular to the line of centres (N)
$\bar{W}_r\bar{W}_t$-non-dimensional load capacity, $\bar{W}_{r,t} = W_{r,t}C^2/\eta UR^2L$
ε -eccentricity ratio, e/C
ε_1 Φ_1 – perturbation parameters
η- coefficient of absolute viscosity of lubricant (Ns/m^2)
θ,$\bar{z}$ -non-dimensional co-ordinates, $\theta = \frac{x}{R}, \bar{z} = z/L$,θ measured from line of centre
θ^* -co-ordinate in the circumferential direction measured from centre of the groove.
$\theta_1\theta_2$ -angular coordinates at which the film cavitates and reforms, respectively
λ- Whirl ratio, $\lambda = \omega_p/\omega$
t- non-dimensional time, $\tau=\omega_p t$

ISSN 2179-3956

Φ- attitude angle(rad)
ψ- assumed attitude angle
ω- journal rotational speed (rad/s)
ω_p frequency of journal vibration(rad/sec)
$( )_0$ Steady state value